Brain Tumour Isolation in MRI Images Based on Statistical Properties and Morphological Process Techniques

Article in Journal of Physics Conference Series · July 2019

DOI: 10.1088/1742-6596/1279/1/012018

3 authors:

Mohammed J. Alwazzan
Al-karkh university of science

Mohammed A Ismael
Al-Hussain University College

Moaid K Hussain
Al-Hussain University College

Journal of Physics: Conference Series

PAPER • OPEN ACCESS

Brain Tumour Isolation in MRI Images Based on Statistical Properties and Morphological Process Techniques

To cite this article: Mohammed J. Alwazzan *et al* 2019 *J. Phys.: Conf. Ser.* **1279** 012018

IOP Conf. Series: Journal of Physics: Conf. Series **1279** (2019) 012018 doi:10.1088/1742-6596/1279/1/012018

Brain Tumour Isolation in MRI Images Based on Statistical Properties and Morphological Process Techniques

Mohammed J. Alwazzan*, Mohammed A. Ismael and Moaid K. Hussain

AL-Hussain University College, Karbala, Iraq.
* dr.mohammedjamal@huciraq.edu.iq

Abstract. With the great development in medical image processing that has been achieved recently, it has become an integral part of diagnostic tools and treatment tools attached to medical imaging devices such as the magnetic resonance imaging (MRI) device. In this paper, we propose an algorithm to extract tumours from MRI images using the MATLAB environment. MRI images were enhanced using different filters, such as the median filter and Wiener's filter. The best results were obtained via Wiener's filter. The k-mean method was used as a key step in the proposed algorithm, then morphology processes were applied and a threshold was proposed based on the statistical properties of the image (standard deviation, maximum and minimum values) to obtain the tumour area. The experimental results obtained by applying the proposed algorithm and DICE coefficient test on different MRI angles (axial, sagittal and coronal) indicate high accuracy was achieved in tumour isolation.

1 Introduction

The nervous system is divided into two main parts: the central nervous system and peripheral nervous system. The central nervous system consists of the brain, its largest part, and spinal cord [1]. The brain is a soft mass of spongy cells protected by: the bones of the skull, three layers of thin tissue called meninges and cerebrospinal fluid. Anatomically, the brain is divided into several sections, which are the forebrain, diencephalon and mid brain [2].

Brain cancer is one of the most serious types of cancer [3]. There are two main types of brain cancer: primary cancer and secondary cancer. Primary brain cancer starts in the brain itself, while secondary brain cancer starts anywhere in the body then travels to the brain [4]. These tumours may be benign or malignant, and can grow rapidly [5]. There are many causes that can lead to brain cancer; some of the genetic conditions which can increase the risk of brain cancer, include: von Hepel-Lindo syndrome, Li-Fraumeni syndrome, and Turcot syndrome. Lymphoma can appear in the brains of people with weak immune systems, sometimes as the result of the Epstein-Barr virus [6, 7]. Other why may cause brain cancer include: exposure to radiation or energy sources, severe head injuries, and tobacco smoking [8- 10]. Magnetic resonance imaging (MRI) images consist of columns and rows of a matrix. When an image is taken the signals from the body are distributed on these pixels according to their distribution in the body [11]. MRI images can be classified according to the angle image was taken at. An image taken from the top of the head (top of head to chin) is called an axial image, while sideways image called sagittal (from ear to ear) is referred to as a called sagittal image. Finally, an image taken from the back (back of head to front) is called a coronal image [12]. Figure 1 represented the planes of an MRI according to angle image was taken from.

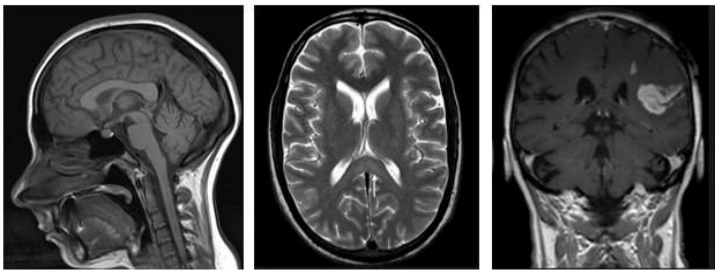

(a) (b) (c)

Figure 1: Different angles of an MRI: (a) sagittal, (b) axial and (c) coronal.

Given the great amount of development in the medical image processing field, image processing techniques have become a substantial part of the MRI devices, starting with such simple operations as contrast adjustment and edge detection and ending with image segmentation algorithms and 3D rendering [13].Nowadays, brain tumour segmentation via MRI methods can be divided into three main categories, including the manual, semi-automatic, and fully-automatic segmentations [14]. The most important factor in brain tumour segmentation is tumour brightness [15]. The use of ionizing radiation for imaging has increased dramatically in recent years but is also accompanied by some risks [11]. Unfortunately, improving the quality of MRI images always means increasing the radiation dose of the patient, which in turn increases the risk of brain tissues damage [16]. For this reasons, image enhancement techniques are very important as a key step in the diagnosis, isolation and interpretation of brain tumours [17].

2 Methodology

The research presented here is based on the application of a series of steps to guarantee automatic segmentation and isolation of the tumour area. The basic steps include the following:
Step one: Read the input MRI image.
Step two: Image enhancement through the use of difference filters (median filter and Wiener's filter).
Step three: Convert the image from RGB colour space to L*a*b* colour space.
Step four: Apply a k-mean classification to a*b* colour space.
Step five: Create six matrices representing the brain features, background and tumour area.
Step six: Apply the proposed threshold to the brain area matrix, where the proposed threshold is

$$T = 2\alpha - \min + (255 - \max) \quad , \qquad (1)$$

where α is the standard deviation of the brain area matrix, and min and max are the minimum and maximum values, respectively.
Step seven: Generate image segmentation (binary image) by using the proposed threshold.

$$g(x,y) = \begin{cases} 255 & if \;\; f(x,y) \geq T \\ 0 & if \;\; f(x,y) < T \end{cases} \qquad (2)$$

Step eight: Apply morphological structuring elements using the MATLAB environment.
Step nine: Dispose of unwanted pixels.
Step ten: Isolate the tumour area.

3 Results and discussion

Image enhancement techniques are one of the most important stages in the analysis and diagnosis of MRI images [17]. These technologies contribute to increasing the clarity of the image and enhance it. Many filters (median filter and Wiener filter) were applied to different angles of the MRI images; the experimental results indicate that the filter that performed well was Wiener filter, as shown in Figures 2, 3 and 4. The images resulting from the use of this filter increased the contrast and strengthened the features. Tables 1 and 2 present the statistical properties of the different imaging angles used in MRIs.

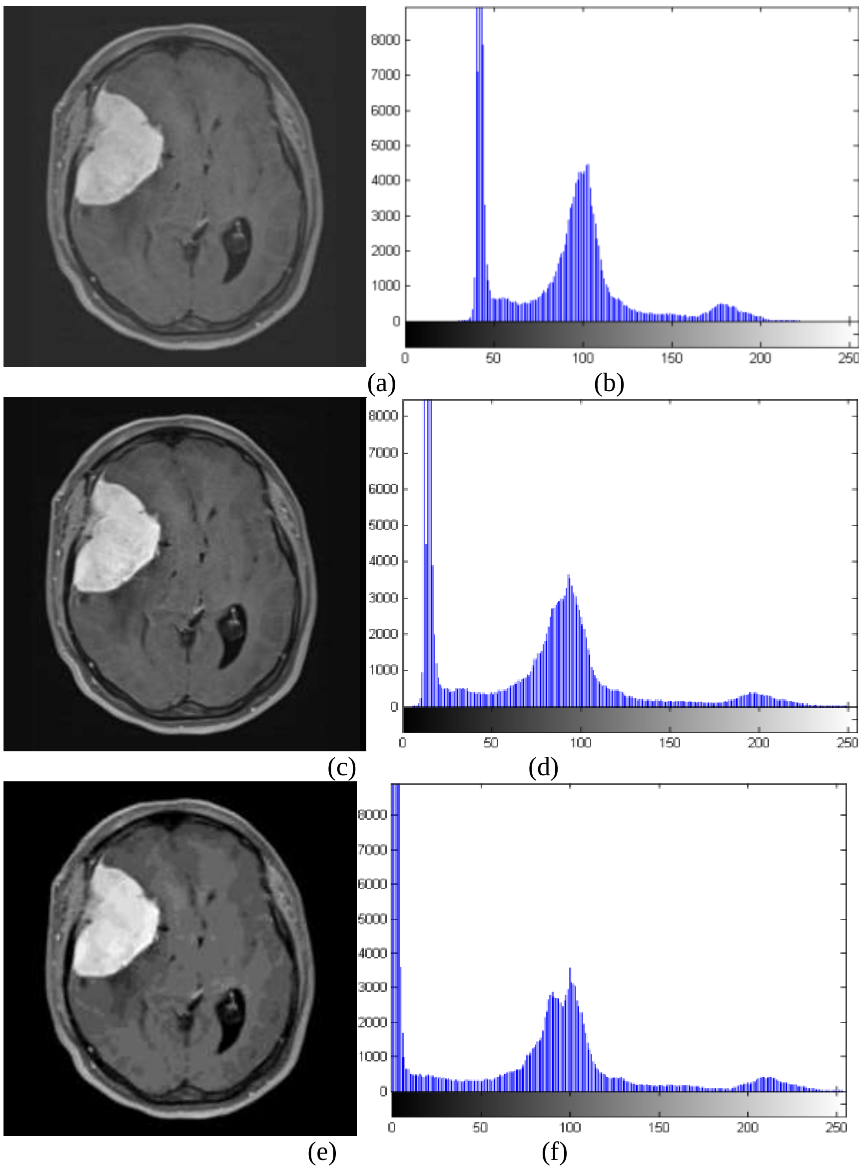

Figure 2: MRI image enhancement of an axial image: (a) Original image, (b) Histogram of Original image, (c) Median filter result, (d) Histogram of Median filter result, (e) Wiener's filter result and (f) Histogram of Wiener's filter result.

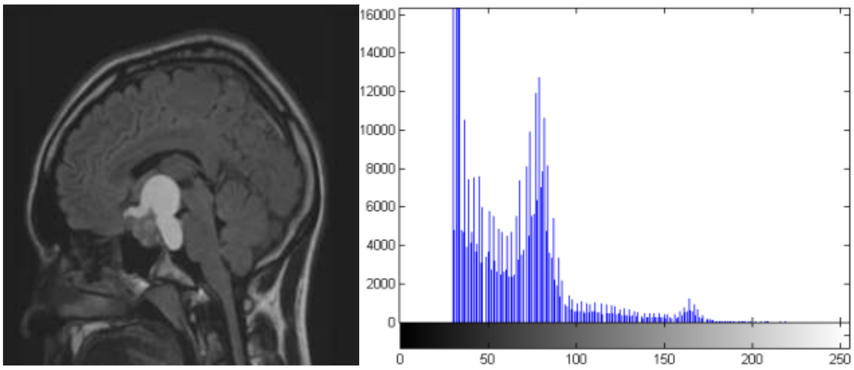

(a) (b)

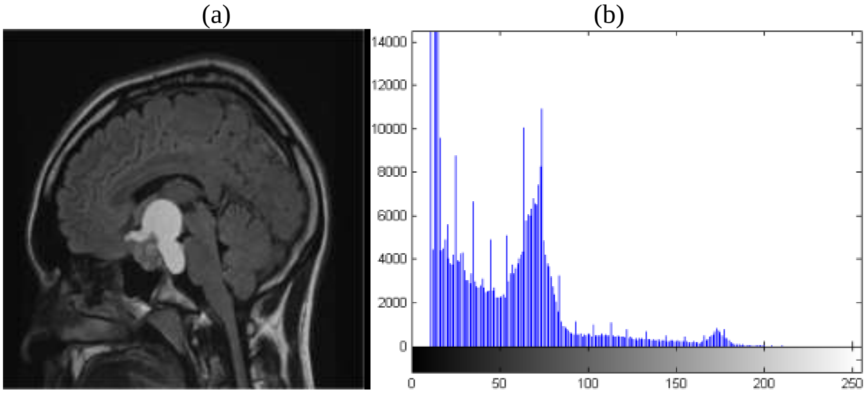

(c) (d)

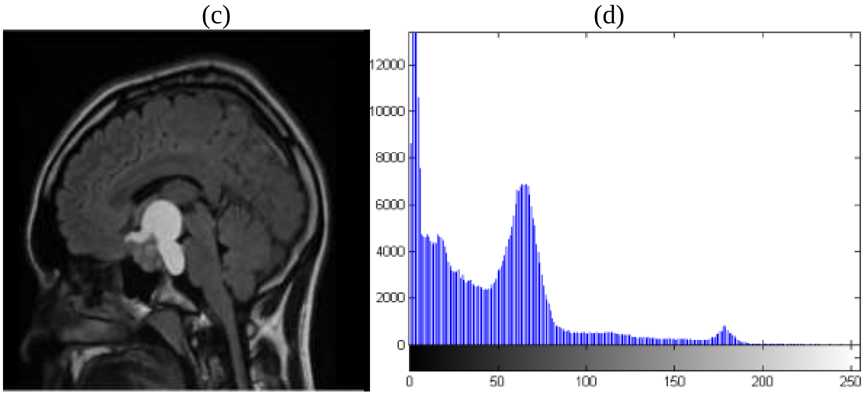

(f) (f)

Figure 3: MRI image enhancement of a sagittal image: (a) Original image, (b) Histogram of Original image, (c) Median filter result, (d) Histogram of Median filter result, (e) Wiener's filter result and (f) Histogram of Wiener's filter result.

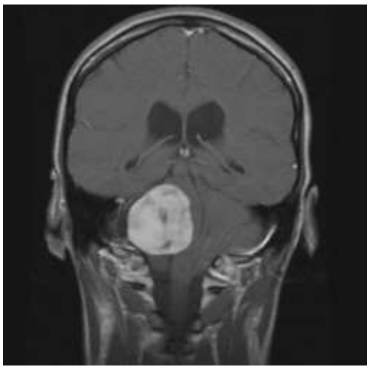

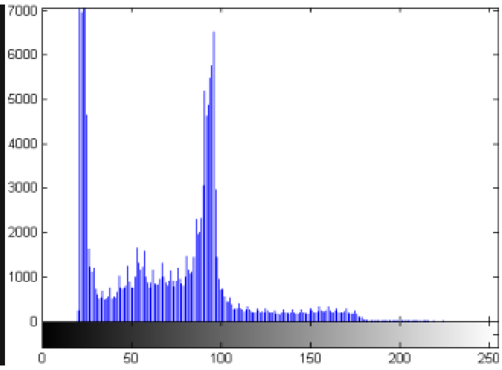

(a) **(b)**

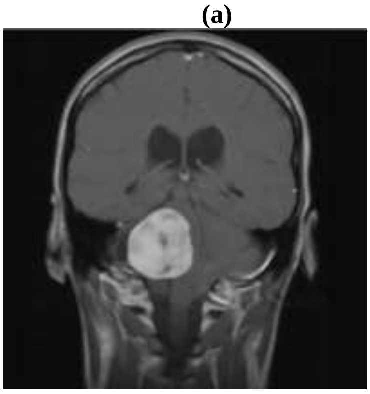

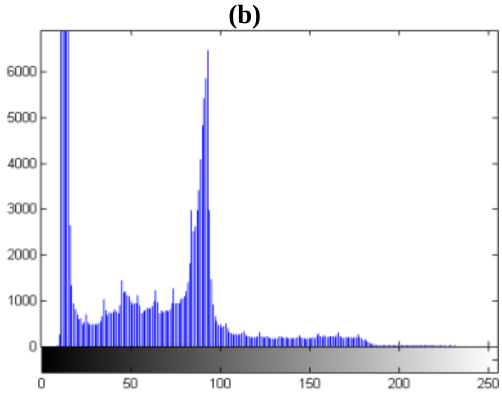

(c) **(d)**

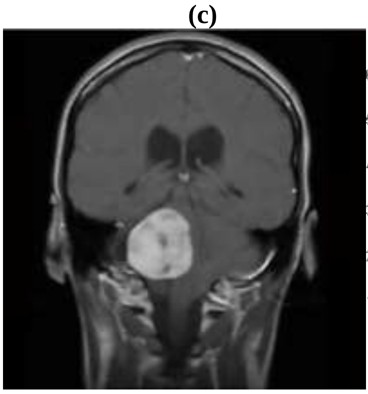

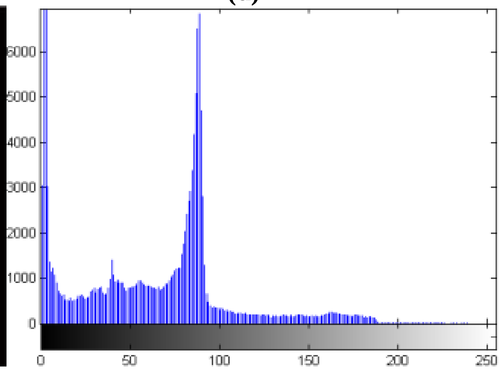

(e) **(f)**

Figure 4: MRI image enhancement of a coronal image: (a) Original image, (b) Histogram of Original image, (c) Median filter result, (d) Histogram of Median filter result, (e) Wiener's filter result and (f) Histogram of Wiener's filter result.

Table 1. Statistical properties of the axial image.

Images	Min	Max	Mean	Standard Deviation
Original image	30	222	75.93	38.18
Median Filter	6	249	59.92	50.97
Wiener Filter	0	253	56.94	58.95

IOP Conf. Series: Journal of Physics: Conf. Series **1279** (2019) 012018 doi:10.1088/1742-6596/1279/1/012018

Table 2: Statistical properties of the sagittal image.

Images	Min	Max	Mean	Standard Deviation
Original image	24	226	53.58	31.87
Median Filter	11	238	44.62	35.84
Wiener Filter	0	250	37.06	39.51

Table 3: Statistical properties of the coronal image

Images	Min	Max	Mean	Standard Deviation
Original image	20	224	60.25	38.58
Median Filter	9	231	53.92	42.26
Wiener Filter	0	239	47.32	45.94

From these tables, it is possible to note that the standard deviation increased after each step (filter). This increase allows for the increased contrast in the MRI, which will provide a good classification of the brain's features, therefore isolating the tumour area correctly.
While applying the k-mean algorithm and Otsu threshold segmentation on the different angles of MRI images, we noticed that a tumour was inaccurate isolated as healthy tissue and that other tissues were incorrectly shown in figures 5 (b), 6 (b) and 7 (b).

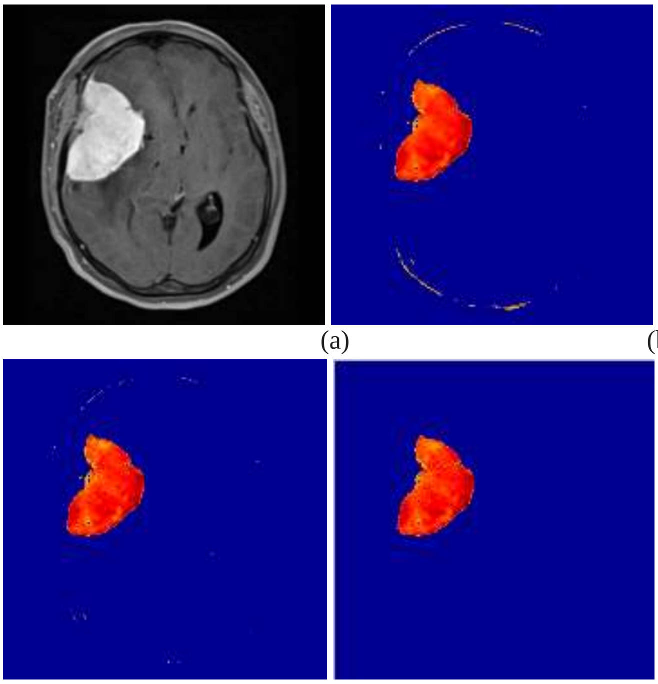

(a) (b)

(c) (d)

Figure 5: Axial image. a) Original image after applying Wiener filter, (b) Otsu segmentation result, (c) Proposed threshold result, (d) Final tumour isolated.

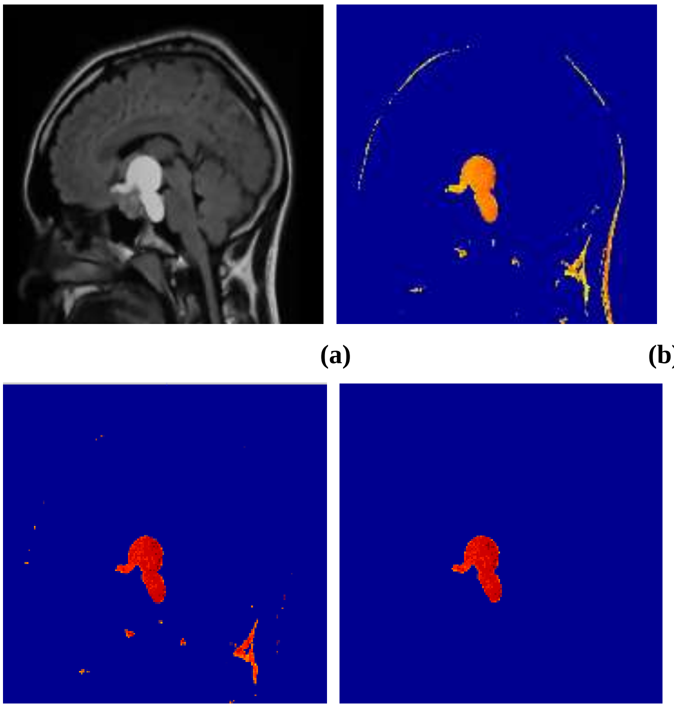

(a) **(b)**

(c) **(d)**

Figure 6: Sagittal image. a) Original image after applying Wiener filter, (b) Otsu segmentation result, (c) Proposed threshold result, (d) Final tumour isolated**.**

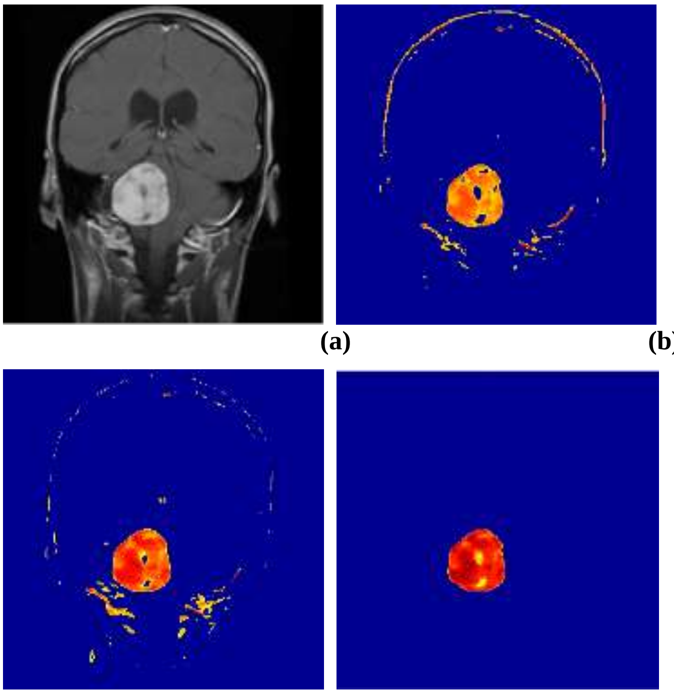

(a) **(b)**

(c) **(d)**

Figure 7: Coronal image. a) Original image after applying Wiener filter, (b) Otsu segmentation result, (c) Proposed threshold result, (d) Final tumour isolated

In figures 5 (d), 6 (d) and 7 (d), we were able to extract the tumour region in the MRI images at different angles automatically without removing the skull edges. As is known, removing the skull's edges in MRI images is a key step in tumour isolation [18]. However, here, removing the skull's edges has been excluded as a basic step in tumour isolation by using the proposed threshold, thus reducing the implementation time, which is a priority in our research. In Figures 5 (c), 6 (c) and 7 (c), the tumour area represents the largest vehicle, but some elements representing unwanted areas appeared after the implementation of the proposed threshold. These areas are eliminated by applying the associated vehicle algorithm and selecting the larger vehicle representing the tumour area. By observing the tumour images and experimental results of the DICE coefficient test shown in Table 4, we note that we extracted the tumour area with high accuracy.

Table 4: Results of the DICE coefficient test.

Elements	DICE of k-mean	DICE of proposed algorithm
Axial view	0.64	0.76
Coronal view	0.69	0.81
Sagittal view	0.71	0.82

4 Conclusion

In this paper, a new algorithm was proposed to isolate brain tumours in MRI images using different image angles (axial, sagittal and coronal). Several technologies were used in this algorithm due to the complexity of the MRI images and the difficulty in extracting the desired tumour area. The main step of the proposed algorithm is to enhance the MRI images using digital filtering techniques to increase the images contrast. It has been shown that Wiener's filter provides the highest contrast. The proposed threshold, which is based on statistical characteristics, gives provides tumour segmentation in MRI images that is better than that provided by the Otsu threshold due to its good performance with high-contrast MRI images. The proposed threshold does not segment the entire tumour, i.e., unwanted pixels appear due to the similarity in brightness between them and the tumour area. Despite the relatively large implementation time, we were able to extract the tumour area with high accuracy.

References

[1] Ghysen, A. 2003. International Journal of Developmental Biology, 47(7), 555-562.
[2] Shaw, L. 2005. Nelson Thornes Ltd, Cheltenham, United Kingdom.
[3] Thomas, D.G.; and Graham, D.I.E.D. 1995. Springer-Verlag London Limited.
[4] Mustaf, M.; Sali, A.F.; Illzam,E.M.; Sharifa, A.M.; and Nang, M.K. IOSR Journal of Dental and Medical Sciences, 17(3), 41-46.
[5] Alnaami, I.;Sarhan, L.; Alqahtani,A.; Alghamdi,A.; Alkhashrami, S.; Mostafa,O. Biomedical Research, 49(14), 2982-2987.
[6] Gomes, J.; Al Zayadi, A.; Guzman, A. 2011. International Journal of Occupational and Environmental Medicine, 2(2), 82-111.
[7] Neparidze, N.; and Lacy, J. 2014. Clinical Features, and Evolving Treatments. Clinical Advances in Hematology & Oncology, 12(6), 358-371.
[8] Kan, P.; Simonsen, S.E.; Lyon, J.L.; and Kestle, J.R. 2007. Journal of Neuro-Oncology, 86(1), 71-78.
[9] Magnavita, N.; Placentino, R.A.; Mei' D.; Ferraro, D.; and Trapani, G. D. 2003. Neurological Sciences, 24, 31–33.
[10] Etxeberria، J.; Roman, E. S.; Burgui,R.; Guevara, M.; Iribas,C.M.; Urbina , M.J.; and Ardanaz E. 2015.Brain and Central Nervous System Cancer Incidence in Navarre (Spain), 1973-2008 and Projections for 2014. Journal of Cancer, 6, 177-183.
[11] Dekker, A.J.;Sijbers, J. 2014. A Review. Physica Medica, 30(7), 725-741.
[12] Yadav,P.; Jantre,M.; and Thakkar, D. 2015. Medical Journal of Dr. D.Y. Patil University, 8(6), 751-759.
[13] Kalaiselvi, T.;Sriramakrishnan, P.; and Somasundaram, K. 2017. Survey of using GPU CUDA. Informatics in Medicine Unlocked, 9(1), 133-144.
[14] Khan, A.M.; and Ravi. S. 2013. Journal of Soft Computing and Engineering, 3(4), 84-92.
[15] Kaur, H.; Kaur, G.; and Kaur' B. 2014. International Journal of Electrical, Electronics and Computer Systems (IJEECS). 2(5), 78-82.
[16] Aquino, C.; Woolen, S.; and Steenburg, S. D. 2015. Emergency Radiology, 22(1), 65-78.
[17] Verma, K.;Mehrotra, A.;Pandey, V.; and Singh, S. International Journal of Advanced Research in Electrical, Electronics and Instrumentation Engineering, 2(4), 1611-1615.
[18] P. Kalavathi, P.; and Prasath, V. B. 2016. Journal of Digital Imaging, 29(3): 365–379.